05

Design of NiMnGaFe alloys with high-temperature superelasticity

© E.E. Timofeeva, E.Yu. Panchenko, M.S. Dmitrienko, E.I. Yanushonite, I.D. Fatkullin, Y.I. Chumlyakov

Tomsk State University, Tomsk, Russia
E-mail: timofeeva_katie@mail.ru

Received January 27, 2025
Revised February 19, 2025
Accepted March 8, 2025

The effect of chemical composition on the microstructure, high-temperature superelasticity and strength properties of martensite has been studied on the $Ni_2MnGa-Fe$ polycrystals. The $Ni_{52}Mn_{17}Ga_{21}Fe_{10}$ and $Ni_{56}Mn_9Ga_{19}Fe_{16}$ (at.%) alloys contain a large amount of the γ-phase (25 to 60 %) which prevents the superelasticity. High-temperature superelasticity in compression was found in the $Ni_{56}Mn_{10}Ga_{25}Fe_9$ polycrystals free of the γ-phase. Transition from polycrystals to single crystals (with close composition of $Ni_{54}Mn_{12}Ga_{25}Fe_9$) results in a significant increase in the martensite strength properties (from 720 to 1450 MPa) due to selecting the compression axis along the high-strength [001]-direction with maintaining the plasticity of 19 % and high-temperature superelasticity.

Keywords: Heusler alloys, martensitic transformation, high-temperature superelasticity, NiMnGaFe, single crystals, γ-phase.

DOI: 10.61011/TPL.2025.06.61289.20269

Designing shape-memory alloys includes obtaining preset parameters of the shape-memory effect (SME) and superelasticity (SE): a certain range of operating temperatures, large reversible strain, narrow or wide stress hysteresis, high cyclic stability, etc. Among the important performance characteristics there are high temperatures of the SME and SE. As per [1], high-temperature alloys are those that exhibit SME and SE at temperatures above 373 K (100 °C), which will allow these alloys to be utilized in the aerospace and automotive industries. When considering functional properties of high-temperature alloys, many researchers pay more attention to the SME. At the same time, there are significantly less studies devoted to high-temperature SE, which is determined by difficult conditions for observing this effect. This requires not only high temperatures of martensitic transformations (MT), but also high strength characteristics of martensite and austenite and low energy losses (low dissipation energy), and, hence, high resistance to the plastic deformation [1]. Otherwise, even if the alloy exhibits high-temperature SME, either the range of SE will be narrow or SE will be accompanied by a plastic flow, significant degradation and irreversibility [2].

Scientific interest in designing high-temperature shape-memory alloys has been steadily increasing over the past 20 years. At the same time, the number of studies on Heusler alloys, intermetallides with chemical formula X_2YZ (X and Y are the transition group elements, and Z are main group elements) is increasing [3,4]. The most prominent representatives of Heusler alloys are the Ni_2MnGa alloys (with composition varying with deviating from stoichiometry). In recent years, the $Ni_2MnGaFe$ alloys have been actively studied; it has been shown that doping with Fe significantly improves the alloy properties, including an increase in ductility of brittle Ni_2MnGa [5–9]. However, designing such alloys faces a great number of difficulties. For instance, variations in the chemical composition often allow increasing temperature M_s (MT onset in cooling) but cause a loss of functionality due to releasing a large number of secondary phases that do not undergo MT, reduce the alloy strength, lead to a loss of SE, and so on. A number of the Ni_2MnGa chemical compositions are known, where MT gets realized at high temperatures [5–7]; however, SE in these alloys remains almost unstudied. The authors are aware of only two papers [8,9] providing examples of SE loops on alloys with compositions close to $Ni_{50}Mn_{25}Ga_{20}Fe_5$ (at. %) and fairly low temperature M_s (about 300 K) of the MT. Therefore, the goal of this study was to investigate the microstructure, high-temperature SE and strength properties of martensite under compressive with varying chemical compositions in high-temperature polycrystalline and single crystals of the $Ni_2MnGa-Fe$ alloys.

Based on the literature analysis, chemical compositions of the $Ni_2MnGa-Fe$ alloys were selected (see the Table and Fig. 1). As shown in [10,11], temperature M_s increases with increasing electron concentration e/a; therefore, compositions with $e/a > 7.7$ were chosen. The electron concentration was calculated taking into account the valence electrons' configuration and number per atom [11]. To achieve high MT temperatures, alloys with the Ni concentration of 50 to 56 at.% [6,12,13] and Ga concentration not less than 19 at.% [14] were selected.

Polycrystals of alloys $Ni_{56}Mn_{10}Ga_{25}Fe_9$ (at.%) (MnFe-9), $Ni_{52}Mn_{17}Ga_{21}Fe_{10}$ (at.%) (MnFe-10), and $Ni_{56}Mn_9Ga_{19}Fe_{16}$ (at.%) (MnFe-16) were produced by electric arc melting from high-purity components. Single crystals of $Ni_{54}Mn_{12}Ga_{25}Fe_9$ were grown by the Bridgman method; the samples were cut so that the compression

Chemical composition of alloys (nominal and actual, see Fig. 1), γ-phase content and chemical composition, MT temperatures in cooling and heating, data on the presence of SE (sorting by increasing electron concentration e/a)

Parameter		Alloy		
		MnFe-9	MnFe-10	MnFe-16
Nominal composition, at.%	Ni	56	52	56
	Mn	10	17	9
	Ga	25	21	19
	Fe	9	10	16
Matrix composition, at.%	Ni	56.4	54.3	54.3
	Mn	10.0	14.1	11.2
	Ga	24.6	22.0	23.0
	Fe	9.0	9.6	11.5
γ-phase composition, at.%	Ni	–	57.1	55.6
	Mn	–	10.7	7.6
	Ga	–	15.2	15.6
	Fe	–	17.0	21.2
γ-phase, %		N/A	25–30	55–60
e/a		7.77	7.82	8.08
SE		+	–	–
M_s, K		423	423	365
M_f,K		391	397	349
A_s, K		405	404	355
A_f, K		435	428	368

axis was parallel to the [001] direction. Chemical composition was studied by energy-dispersive X-ray (EDX) spectroscopy on the TESCAN VEGA 3 scanning electron microscope with the error of 5 at.%. Temperature dependence of electrical resistance was used to determine MT temperatures. Optical metallography data was obtained using the Keyence VHX-2000 digital microscope at 295 K after the oriented martensite stabilization by external loading. The SE curves were obtained on samples $3 \times 3 \times 6$ mm in size by using the Instron 5969 testing machine with the strain rate of $10^{-3}\,\mathrm{s}^{-1}$. In the data analysis, the measuring errors were as follows: ± 0.1 % for strain, ± 1 K for temperature, and ± 2 MPa for stress.

All the alloys under study exhibited the thermoelastic MTs. Temperatures of the forward (M_s, M_f) and reverse (A_s, A_f) MTs are given in the Table. Temperatures M_s for all the alloys range from 365 to 423 K. The MT temperatures in these materials are extremely sensitive to precipitation of secondary phases and variations in chemical composition. In the MnFe-9 and MnFe-10 alloys whose Fe contents in matrix are close to each other, temperatures M_s are also close, while in the MnFe-16 alloys where the Fe content is higher, temperatures are lower; this complies with [5–8]. Papers [5–9] have shown that in the NiMnGaFe alloys MT occurs from $L2_1$-austenite to tetragonal unmodulated martensite through intermediate layered modulated martensite 10M and/or 14M. Fig. 1 shows the results of energy dispersive X-ray (EDX) maps of the alloys' surfaces and chemical compositions with elemental distribution. Relevant data are given in the Table.

The MnFe-10 and MnFe-16 alloys contain a large volume fraction (25–30 and 55–60 %) of the γ-phase (fcc lattice). The γ-phase composition depends on the nominal alloy composition; however, in all cases the γ-phase is enriched in Fe and depleted in Mn and Ga (see the Table), which complies with [5]. The γ-phase precipitation primarily leads to strong variations in the matrix chemical composition with respect to the nominal composition.

The secondary γ-phase precipitates in the form of large shapeless regions 20–100 μm in size in MnFe-10 and 50–500 μm in MnFe-16. The γ-phase regions do not undergo MT, reduce the volume fraction of the matrix undergoing MT, and may induce formation of martensite variants different from the main-orientation variant of stress martensite (Fig. 1, *b*). In this case, stress-induced MT proceeds through multivariant nucleation of martensite crystals between the γ-phase regions with interaction between different martensite variants; this was also found in [5]. High-temperature annealing at 1273 K for 1–4 h did not promote dissolution of the γ-phase.

In the MnFe-10 and MnFe-16 alloys, such a two-phase microstructure provides high critical stresses σ_{cr} which are necessary both for reorientation of martensite variants at $T < M_s$ (at least 200 MPa) and for formation of oriented martensite at $T > A_f$ (250–280 MPa at $T = A_f + 30$ K) (Fig. 2). It is worthy to note that, during the MT, the γ-phase may undergo plastic deformation and significantly contribute to the dissipation energy. Paper [15] shows that the γ-phase yield strength in the Heusler alloy NiFeGa is low and amounts to only 260 MPa at 373 K, which is comparable to the stress level at which MT occurs. In the MnFe-10 and MnFe-16 alloys, the presence of a large volume fraction of plastic γ-phase leads to a low martensite yield strength σ_{cr}^M: 800–860 MPa at 295 K (Fig. 2). High critical stresses σ_{cr} necessary for the martensite formation, large volume fraction of plastic γ-phase and low martensite yield strength σ_{cr}^M prevent the SE (i. e., obtaining reversible strain upon unloading) in the MnFe-10 and MnFe-16 alloys (Fig. 2). At the temperatures above the finish temperature of reverse MT (A_f), the entire specified strain is irreversible. Similar results were obtained in [16] where it was shown that in the NiMnGaFe alloys with high Fe content and large γ-phase volume fraction the reversibility of given strain is low.

In the MnFe-9 alloy, no γ-phase was detected (Fig. 1, *a*); the matrix chemical composition was homogeneous and close to the nominal (see the Table). The absence of the secondary phase provides low stresses of the martensite variants reorientation at $T < M_s$ (below 30–50 MPa) and low stresses of the oriented martensite formation at $T > A_f$ (150 MPa at $T = A_f + 30$ K) (Fig. 2). Note that the martensite yield strength at 295 K in the MnFe-9 alloys is 720 MPa, which is even lower than in the MnFe-10 and

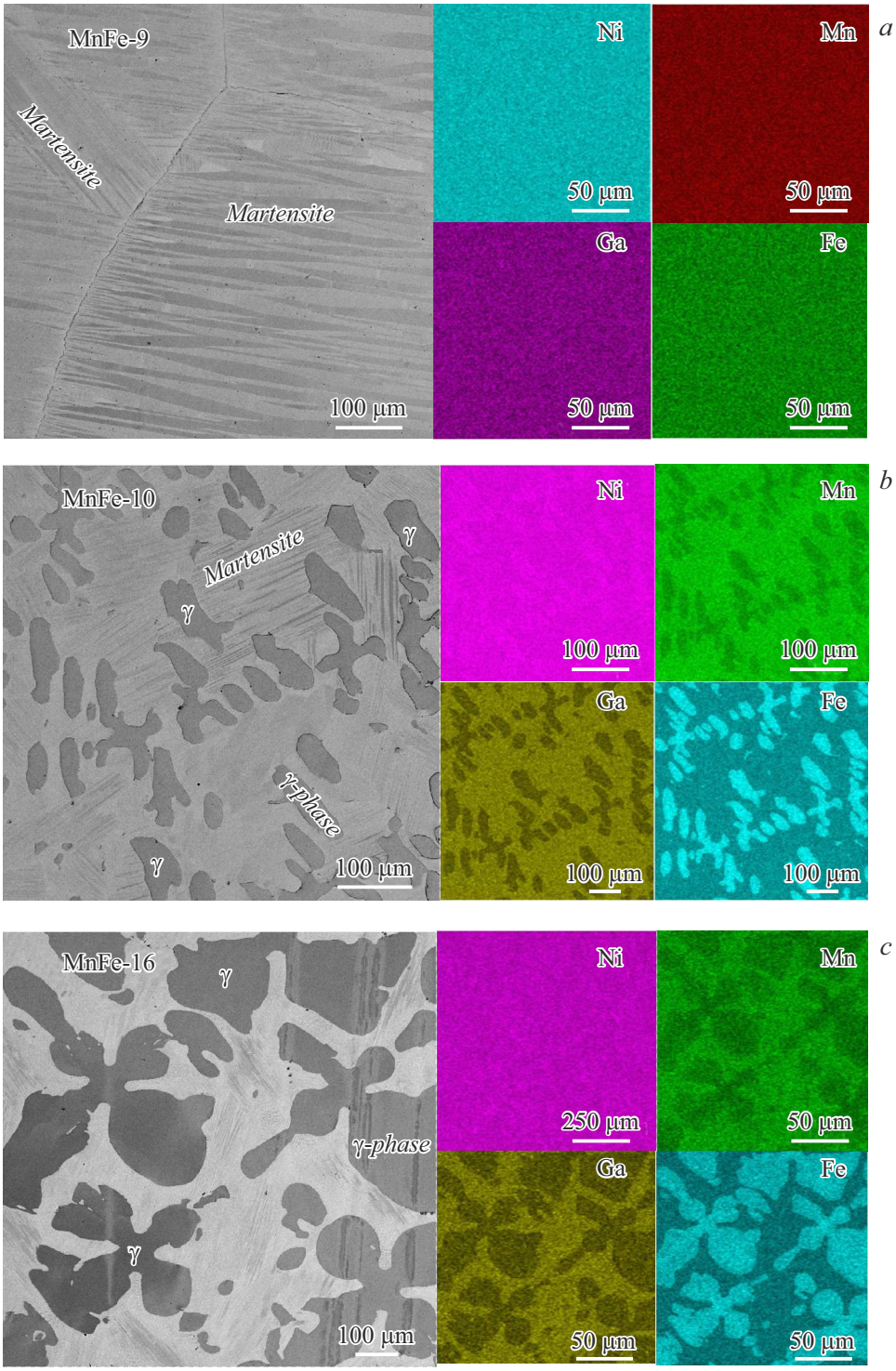

Figure 1. Results of energy dispersive X-ray (EDX) maps of the surface and chemical composition (with elemental distribution) for the MnFe-9 (*a*), MnFe-10 (*b*) and MnFe-16 (*c*) alloys.

MnFe-16 alloys. At the same time, high-temperature SE was detected in the MnFe-9 alloy. The reason why, unlike the MnFe-10 and MnFe-16 alloys, MnFe-9 exhibited SE, is as follows. The MnFe-9 alloys do not contain the γ-phase, while alloys MnFe-10 and MnFe-16 contain a large volume fraction of the γ-phase. Near the γ-phase, non-oriented martensite gets formed; the γ-phase may be plastically deformed during MT and is the main reason for the energy dissipation during MT and absence of reversible strain. Therefore, in the MnFe-9 alloy free of the γ-phase, MT occurs at low stresses (4–8 times lower than the martensite yield strength), whereas in the MnFe-10 and MnFe-16

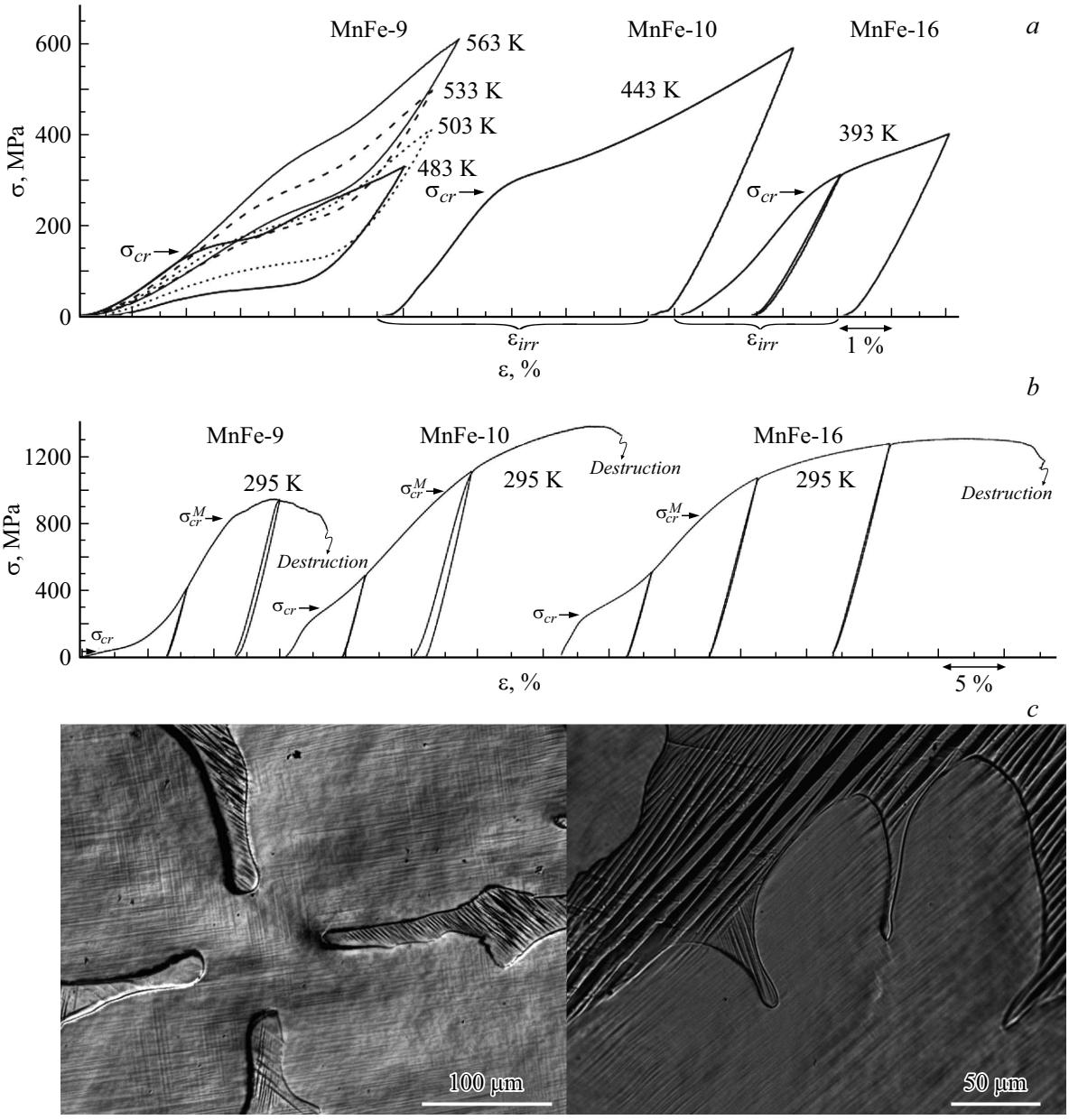

Figure 2. Curves $\sigma(\varepsilon)$ at $T > A_f$ demonstrating the SE or absence of SE (a), and curves at 295 K $< M_s$ demonstrating the martensite strength properties (b) in the MnFe-9, MnFe-10 and MnFe-16 alloys under compression. c — optical metallography data demonstrating the formation of non-oriented martensite near the γ-phase and traces of the γ-phase deformation as exemplified by the MnFe-16 alloys.

alloys the level of martensite formation is only 2–2.5 times lower than the martensite yield strength. Thus, the great importance for SE consists in not only the martensite yield strength but also the critical stresses of stress-induced MT and their relationship.

It is necessary to note high plasticity of all the investigated MnFe-9, MnFe-10 and MnFe-16 alloys. Despite the absence of the γ-phase, the maximum preset prior-to-failure strain in the MnFe-9 alloy is 19.5 % at 295 K. For comparison, in the NiMnGa-based alloys the maximum specified strain under compression is 12 to 20 % [16,17]. An increase in the γ-phase content results in the plasticity increase to 24 % in MnFe-10 and to 36 % in MnFe-16.

It is known that NiMnGa-based alloys, like other Heusler alloys, are characterized by strong anisotropy of properties (the crystal anisotropy parameter is $A = 2C_{44}/(C_{11} - C_{12}) > 10$) [18]. Therefore, to obtain higher functional characteristics, the NiMnGa single crystals are often used. Parameters optimal for the SE under compression in single crystals of Heusler alloys are observed along the [001] orientation which is highly strong in austenite. Under compression, this orientation is characterized not only by the maximum reversible strain, but also by

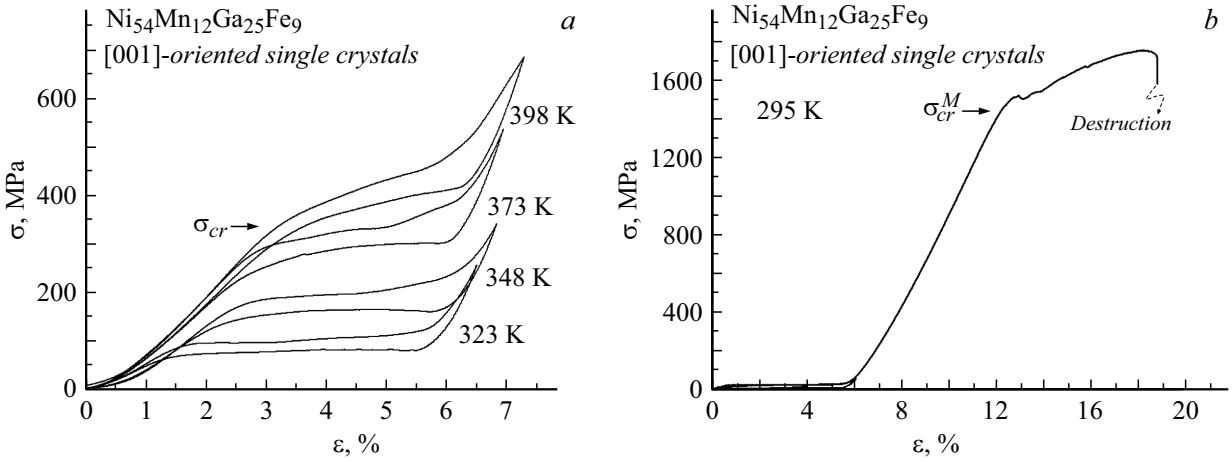

Figure 3. Curves $\sigma(\varepsilon)$ at $T > A_f$ demonstrating the SE (a) and curve $\sigma(\varepsilon)$ at $295\,\mathrm{K} < M_s$ demonstrating the martensite strength properties (b) in the [001]-oriented single crystals of $Ni_{54}Mn_{12}Ga_{25}Fe_9$ (at.%) under compression.

a zero Schmid factor for slip in the $B2(L2_1)$-phase and minimal hysteresis; detwinning of tetragonal martensite crystals during the transformation makes virtually no contribution to the transformation strain along [001] orientation [19,20].

To improve the strength characteristics, extend the SE range, and minimize stress hysteresis, we have obtained in this work single crystals with chemical compositions close to MnFe-9 and cut the samples along the high-strength [001] orientation. Since the possibility of orienting single crystals with the MT temperature above 400 K is limited, the chemical composition was adjusted from $Ni_{56}Mn_{10}Ga_{25}Fe_9$ (MnFe-9) to $Ni_{54}Mn_{12}Ga_{25}Fe_9$ (at.%). In the obtained single crystal, thermoelastic MT starts at 295 K. Under compression along the [001] orientation, SE was revealed in the range of 323 to 398 K. Due to selecting the [001] orientation, the martensite strength characteristics increased by 2 times as compared to the MnFe-9 polycrystals, that is, to 1450 MPa (Fig. 3). Along with this, the stress hysteresis decreased by 5–8 times, i.e. from 110–150 to 20–30 MPa.

The maximum specified prior-to-failure strain is 19 %. To the best of the authors' knowledge, maximum plasticity of the NiMnGa alloys has been found in [17] in $Ni_{54}Mn_{25}Ga_{21}$ and is 20.5 %; however, the yield strength in this case is low and does not exceed 700 MPa. In the obtained $Ni_{54}Mn_{12}Ga_{25}Fe_9$ single crystals, the level of the martensite strength properties is 2 times higher at the same plasticity. Note that the ratio of high plasticity (28 %) to high strength (1700 MPa) was also achieved in [16] in $Ni_{56}Mn_{17}Fe_8Ga_{19}$; however, reversibility of the specified strain in them was low, similarly to MnFe-10 and MnFe-16, because of high γ-phase content.

Thus, alloys based on Ni_2MnGa–Fe were studied, compositions with high MT temperatures were selected, and microstructure, high-temperature SE and strength properties of martensite were studied. It was revealed that the $Ni_{52}Mn_{17}Ga_{21}Fe_{10}$ and $Ni_{56}Mn_9Ga_{19}Fe_{16}$ alloys contain a large amount of the γ-phase (25 to 60 %) that prevents high-temperature SE due to high stresses of martensite formation (200–280 MPa), high energy dissipation during MT, low reversibility of the specified strain, and low martensite yield strength (800–860 MPa). On the contrary, in the $Ni_{56}Mn_{10}Ga_{25}Fe_9$ alloys there is no γ-phase, and martensite formation stresses are lower (100–150 MPa, which is 4–8 times lower than the martensite yield strength, i.e. 720 MPa), which leads to high-temperature SE. Transition from polycrystals to single crystals of the close composition ($Ni_{54}Mn_{12}Ga_{25}Fe_9$) results in a significant improvement of the martensite strength properties (from 720 to 1450 MPa) due to selecting the compression axis along the high-strength [001]-direction with maintaining high plasticity of 19 % (up to destruction). In the $Ni_{54}Mn_{12}Ga_{25}Fe_9$ single crystals, SE was detected under compression along the [001] orientation in the range of 323 to 398 K. Based on the studies performed, it may be concluded that, due to formation of a sharp texture along the [001] direction, it is possible to obtain in polycrystals of alloys with a composition close to $Ni_{56}Mn_{10}Ga_{25}Fe_9$ an easy-to-produce material exhibiting high-temperature SE and optimal strength-to-plasticity ratio.

Funding

The study was supported by the Russian Science Foundation (project № 24-19-00242).

Conflict of interests

The authors declare that they have no conflict of interests.

References

[1] J. Ma, I. Karaman, R.D. Noebe, Int. Mater. Rev., **55**, 257 (2010). DOI: 10.1179/095066010X12646898728363
[2] J.P. Oliveira, R.M. Miranda, N. Schell, F.M. Braz Fernandes, Int. J. Fatigue, **83**, 195 (2016). DOI: 10.1016/j.ijfatigue.2015.10.013

[3] A. Amudhavalli, P. Dharmaraj, M. Manikandan, R. Palanichamy, R.K. Iyakutti, Solid State Sci., **144**, 107307 (2023). DOI: 10.1016/j.solidstatesciences.2023.107307
[4] G. Zhang, H. Hao, Y. Liang, Y. Qiao, S. Bai, H. Liu, H. Luo, J. Magn. Magn. Mater., **584**, 171071 (2023). DOI: 10.1016/j.jmmm.2023.171071
[5] S.Y. Yang, Y. Liu, C.P. Wang, Z. Shi, X.J. Liu, J. Alloys Compd., **560**, 84 (2013). DOI: 10.1016/j.jallcom.2013.01.128
[6] S. Yang, Y. Liu, C. Wang, X. Liu, Acta Mater., **60**, 4255 (2012). DOI: 10.1016/j.actamat.2012.04.029
[7] S.K. Sarkar, A. Biswas, P.D. Babu, S.D. Kaushik, A. Srivastava, V. Siruguri, M. Krishnan, J. Alloys Compd., **586**, 515 (2014). DOI: 10.1016/j.jallcom.2013.10.057
[8] Y. Liu, X. Zhang, J. Liu, D. Xing, H. Shen, D. Chen, J. Sun, Mater. Res., **18**, 61 (2015). DOI 10.1590/1516-1439.325914
[9] Y. Liu, X. Zhang, D. Xing, H. Shen, M. Qian, J. Liu, D. Chen, J. Sun, Mater. Sci. Eng. A, **636**, 157 (2015). DOI: 10.1016/j.msea.2015.03.092
[10] D. Soto, F.A. Hernández, H. Flores-Zúñiga, X.Moya, L. Mañosa, A. Planes, S. Aksoy, M. Acet, T. Krenke, Phys. Rev. B, **77**, 184103 (2008). DOI: 10.1103/PhysRevB.77.184103
[11] V.A. Chernenko, Scripta Mater., **40**, 523 (1999). DOI: 10.1016/S1359-6462(98)00494-1
[12] C. Jiang, G. Feng, S. Gong, H. Xu, Mater. Sci. Eng. A, **342**, 231 (2003). DOI: 10.1016/S0921-5093(02)00288-5
[13] Y. Xin, L. Chai, Rare Met., **33**, 41 (2014). DOI: 10.1007/s12598-013-0081-6
[14] R. Santamarta, E. Cesari, J. Muntasell, J. Font, J. Pons, P. Ochin, Intermetallics, **18**, 977 (2010). DOI: 10.1016/j.intermet.2010.01.016
[15] E.E. Timofeeva, E.Yu. Panchenko, A.S. Eftifeeva, N.Yu. Surikov, A.I. Tagiltsev, I. Kurlevskaya, J. Alloys Compd., **1005**, 176076 (2024). DOI: 10.1016/j.jallcom.2024.176076
[16] Y. Xin, Y. Li, L. Chai, H. Xu, Scripta Mater., **57**, 599 (2007). DOI: 10.1016/j.scriptamat.2007.06.010
[17] H. Xu, Y. Ma, C. Jiang, Appl. Phys. Lett., **82**, 3206 (2003). DOI: 10.1063/1.1572540
[18] L. Dai, J. Cullen, J. Cui, M. Wuttig, Phys. Rev. B, **70**, 054115 (2004). DOI: 10.1103/PhysRevB.70.054115
[19] R.F. Hamilton, H. Sehitoglu, K. Aslantas, C. Efstathiou, H.J. Maier, Acta Mater., **56**, 2231 (2008). DOI: 10.1016/j.actamat.2008.01.007
[20] L. Wei, X. Zhang, J. Liu, L. Geng, AIP Adv., **8**, 055312 (2018). DOI: 10.1063/1.5028212

Translated by EgoTranslating